COMMUNICATION

Check for updates

Magnetic field-responsive graphene oxide photonic liquids†

Yi-Tao Xu,[a] Amanda J. Ackroyd, [ID][a] Arash Momeni,[a] Mohamed Oudah[b] and Mark J. MacLachlan [ID] *[abcd]

Modifying the environment around particles (*e.g.,* introducing a secondary phase or external field) can affect the way they interact and assemble, thereby giving control over the physical properties of a dynamic system. Here, graphene oxide (GO) photonic liquids that respond to a magnetic field are demonstrated for the first time. Magnetic nanoparticles are used to provide a continuous magnetizable liquid environment around the GO liquid crystalline domains. In response to a magnetic field, the alignment of magnetic nanoparticles, coupled with the diamagnetic property of GO nanosheets, drives the reorientation and alignment of the nanosheets, enabling switchable photonic properties using a permanent magnet. This phenomenon is anticipated to be extendable to other relevant photonic systems of shape-anisotropic nanoparticles and may open up opportunities for developing GO-based optical materials and devices.

The ability of many organisms to alter their visible appearance to adapt to diverse environments is a remarkable trait that inspires the development of new materials. Of particular interest are organisms that can alter the size and orientation of photonic structures to control light diffraction or scattering to produce tunable structural colors in response to stimuli.[1–4] Taking inspiration from nature, researchers are developing analogous responsive photonic structures with potential applications in optical devices or sensors[5–9] from block copolymers,[9–12] silica spheres,[13–17] polymer spheres,[5] and other building blocks.[2,7,18–23]

Several species of fish (*e.g.,* koi, tetras, damselfish) appear colorful because of the layered stacks of guanine sheets separated by fluidic cytoplasm in their iridophores.[4,24–26] In particular, these fish can abruptly change the tilt angles (like a

New concepts

Photonic liquids of two-dimensional nanoparticles are emerging photonic systems capable of displaying full-color reflection in various solvents. Since the discovery of photonic properties in suspensions of graphene oxide (GO) in 2014, researchers have developed ways to control the color presented with additives and changing the concentration. However, achieving reversible color switching, which is important for using them in sensors and displays, remains an unsolved challenge. In this study, we exploited magnetic nanoparticles to create a magnetizable liquid environment around GO nanosheets. We observed for the first time that the GO-based suspensions showed reversible color changes in response to a moderate-strength magnetic field. This phenomenon is associated with the reorientation of GO nanosheets, directed by the magnetized ferrofluids, in response to the magnetic field. This study provides important insights for the development of lyotropic magnetic field-responsive photonic systems using shape-anisotropic nanoparticles in a magnetizable liquid environment, and may open up opportunities for broadening the use of GO-based materials in particular for photonic sensors and displays.

venetian blind) or interlayer distances of the iridophores to create a fluid and flamboyant display of color in response to stimuli in a rapidly changing environment.[4,24–26] In a similar way, suspensions of nanosheets such as $H_3Sb_3P_2O_{14}$,[27–29] phosphate,[30–32] titanate,[33] niobate,[34] perovskites[35] and fluoro-hectorite clay[36–38] can also display fluidic photonic properties, as these nanoparticles can form lyotropic liquid crystalline lamellar phases in which the space between nanosheets is filled with solvent molecules. The spacings (*i.e.,* the periodic/interlayer distance) can be regulated to match different wavelengths of visible light by adjusting the nanosheet concentration, resulting in photonic liquids with tunable structural colors spanning the entire visible spectrum.[30,33,36] Producing stimuli-responsive reversible color changes, however, remains challenging in these systems. Controlling the orientation of nanosheets could be a potential direction for developing photonic liquids with controllable color changes, and important for increasing the applicability of photonic liquids in sensors and displays.

Graphene oxide (GO) is a sheet-like substance with oxygen-containing functional groups that help it form stable

[a] *Department of Chemistry, University of British Columbia, 2036 Main Mall, Vancouver, British Columbia V6T 1Z1, Canada. E-mail: mmaclach@chem.ubc.ca*

[b] *Stewart Blusson Quantum Matter Institute, University of British Columbia, 2355 East Mall, Vancouver, British Columbia V6T 1Z1, Canada*

[c] *WPI Nano Life Science Institute, Kanazawa University, Kanazawa 920-1192, Japan*

[d] *Bioproducts Institute, University of British Columbia, 2360 East Mall, Vancouver, British Columbia V6T 1Z3, Canada*

suspensions in water and some non-aqueous solvents.[39] Above a critical concentration, aqueous suspensions of GO nanosheets form a liquid crystalline nematic or lamellar phase.[40,41] It has been observed that the liquid crystalline phases of GO suspensions can produce tunable structural colors by varying the GO concentration.[42] However, to date, other methods to manipulate the color of GO photonic liquids have only been achieved with nanosized additives or applied electric fields,[43–45] and issues such as reversibility and stability, and developing photonic liquids in hydrophobic liquid media also need more investigation.

Magnetic fields are an attractive tool for manipulating the optical properties of GO photonic liquids because they can align particles in a non-invasive and contactless manner; however, this area remains unexplored. The magnetic alignment of GO nanosheets has been documented, though powerful superconducting magnets were required due to the diamagnetic behavior of GO. Furthermore, no structural color was observed in these systems.[46]

Previously, it was shown that non-magnetic particles within a magnetized ferrofluid behave diamagnetically with respect to the surrounding fluid, allowing them to be aligned using a relatively weak magnetic field.[47–49] This differs from the situation of non-magnetic particles in non-magnetic liquid media (e.g., GO in water or organic solvents), where very strong magnetic fields are required to induce magnetic dipole–dipole interactions for particle alignment. Therefore, the use of a magnetic fluid surrounding non-magnetic particles opens up opportunities for controlling the assembly of non-magnetic particles and developing photonic patterns using easily accessible magnetic fields.[7,47–55]

Here, we take advantage of the diamagnetic behavior of GO liquid crystalline domains in a magnetized ferrofluid to develop GO photonic liquids with switchable photonic properties controlled by readily-available permanent magnets. GO nanosheets in a magnetized surrounding environment (i.e., ferrofluid) tend to orient their planes parallel to the field direction, allowing for the on/off switching of structural colors of GO photonic liquids in response to magnetic fields.

GO nanosheets were synthesized using Hummers' method,[44,45,56] and Fe_3O_4 nanoparticles (NPs) were prepared via the coprecipitation method in the presence of polyacrylic acid (see Experimental section in ESI†).[57] GO nanosheets are ~ 0.5 to 6 μm in lateral size and Fe_3O_4 NPs are ~ 5 to 15 nm in diameter (Fig. S1, ESI†). Both the GO and Fe_3O_4 NPs are negatively charged (zeta potential, ~ -39 mV for GO and ~ -22 mV for Fe_3O_4); electrostatic repulsion prevents attachment of the Fe_3O_4 NPs to the GO nanosheets and thus helps them to form a stable hybrid suspension without observable flocculation.

We expect superparamagnetic, single-domain, behaviour for Fe_3O_4 NPs with diameter less than 25 nm,[58] and this is confirmed by magnetization measurements of the Fe_3O_4 NPs (Fig. S1, ESI†). We compared the magnetic susceptibility as a function of temperature measured in zero-field cooling (ZFC) and field-cooling (FC) conditions with an applied field of 1 mT.

In the ZFC susceptibility, we found an increase in magnetization as a function of temperature at low temperature, reaching a maximum value then decreasing with increasing temperature above ~ 90 K. We define this maximum as the blocking temperature (T_B), and above T_B we observed that ZFC and FC curves coincide. For $T < T_B$ we found ferromagnetic behaviour as can be seen for data measured at 2 K showing finite coercivity and remnant magnetization. This implies that the thermal energy is insufficient to induce moment randomization at 2 K so that the nanocrystals show typical ferromagnetic hysteresis loops. The coercivity and remnant magnetization are equal to zero for $T > T_B$, which is demonstrated by the data measured at 300 K. This confirms the superparamagnetic behaviour in the Fe_3O_4 NPs at room temperature.

GO nanosheets and Fe_3O_4 NPs can be transferred from water into hydrophobic solvents by using aminopropylmethyl-siloxane-dimethylsiloxane copolymer [poly(APMS-co-DMS)], a known phase transfer additive,[45,59] allowing for the formation of photonic liquids and ferrofluids in different liquid media (see Experimental section and Fig. S2, ESI†). In water or hydrophobic solvents (e.g., butyl acetate), GO forms photonic liquids with structural colors that span from red to blue in response to changing concentration (Fig. S3, ESI†). That is, the interlayer separation of GO sheets changes with concentration.[42,45] On the other hand, suspensions of Fe_3O_4 NPs alone in different liquid media do not exhibit any reflection colors, regardless of the presence of a magnetic field (Fig. S3, ESI†). We mainly focused on GO-based non-aqueous photonic liquids for our experiments because they are more stable than the corresponding aqueous photonic liquids (Fig. S4, ESI†). Although the reasons for the enhanced stability of GO photonic liquids in hydrophobic solvents is not yet fully understood, it is possible that solvents with low dielectric polarizability can better prevent the degradation of GO suspensions and the reactions between GO and solvents.[45] Moreover, it's possible that water reacts with functional groups on the surface of GO over time, modifying intersheet interactions.

Addition of the Fe_3O_4 NPs to GO photonic liquids led to a visible blue-shift of the reflection color (Fig. S5, ESI†), in agreement with our previous work on hybrid photonic liquids based on GO and foreign nanoparticle additives.[44,45] This is attributed to the depletion interaction between particles, an entropy-driven process that minimizes the excluded volume of GO and increases the free volume for depletant nanoparticles,[44,45,60,61] resulting in a decrease in the intersheet separation when Fe_3O_4 NPs are added. Thus, we were able to tune the reflection color of GO–Fe_3O_4 photonic liquids by altering the Fe_3O_4:GO ratio.

A blue-colored photonic liquid containing GO nanosheets and Fe_3O_4 NPs (GO, ~ 4 mg mL^{-1}; Fe_3O_4:GO mass ratio, $\sim 1.3:1$; in butyl acetate) shown in Fig. 1 was used to investigate the magnetoresponsive properties (responsiveness for the red samples is shown in Fig. S6, ESI†). The Fe_3O_4 concentration used ensured a magnetized surrounding environment for the experiments. In the absence of a magnetic field, the blue color of the photonic liquid in a cuvette can be observed from both the front and sides (Fig. 1d). This phenomenon could be
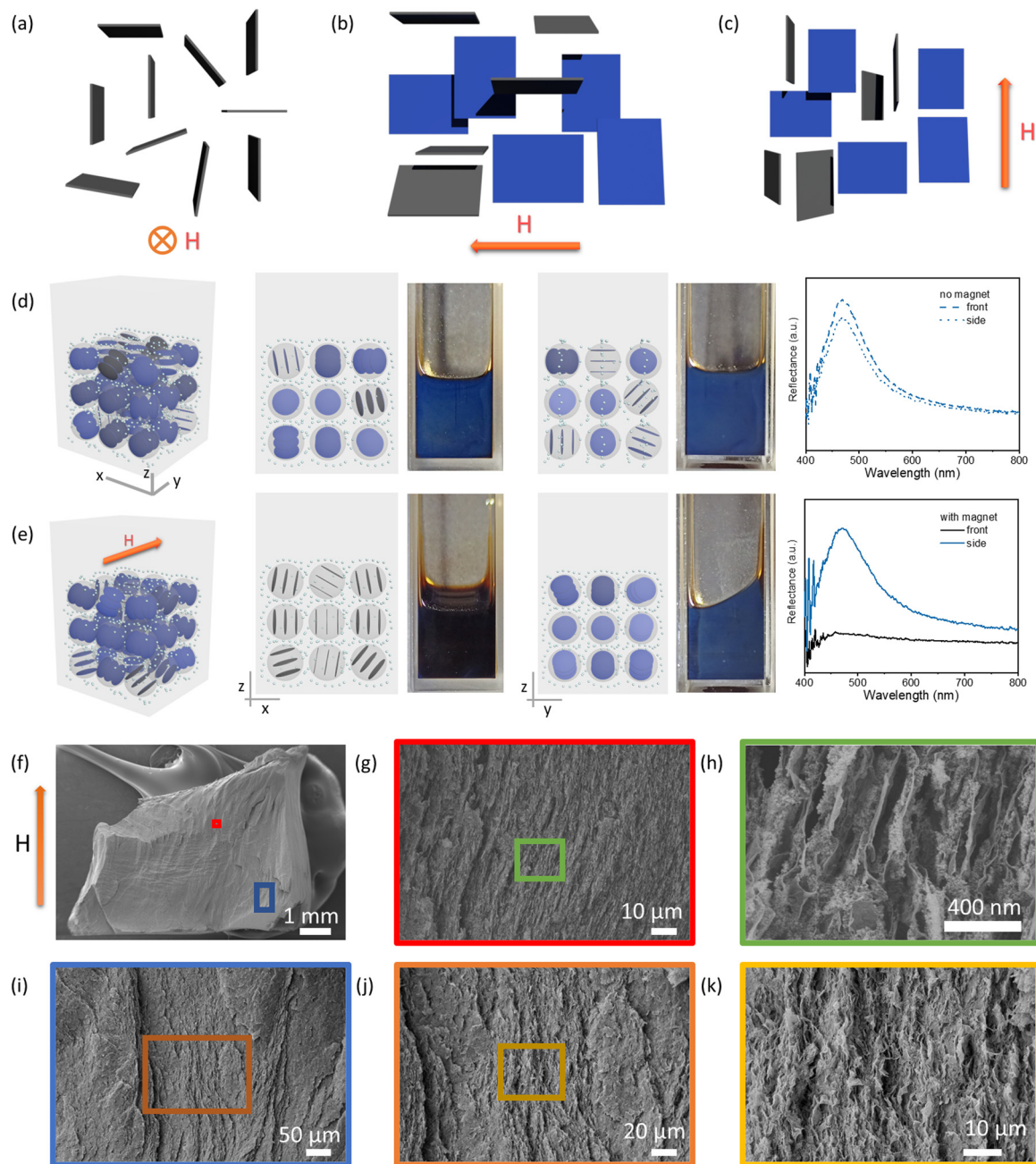
Fig. 1 (a)–(c) Possible orientations of GO nanosheets in the magnetized ferrofluid. The nanosheets are parallel to the field direction with a distribution of degenerate orientations. When the magnetic field is directed into the page (a), the nanosheets orient with their lateral planes parallel to the field, and no nanosheets are perpendicular to the viewing direction. When the magnetic field is pointed to the left (b) or in the upright direction (c), some nanosheets are not only parallel to the field direction but also perpendicular to the viewing direction, which contributes to the visible light reflection. (d) and (e) Front and side view of a blue photonic liquid and its corresponding reflection spectra without (d) and with (e) a magnet positioned behind the cuvette (only a blue photonic liquid is shown here; for the same effect observed for a red photonic liquid, see Fig. S6, ESI†); models near the sample images show the possible domain orientation of GO in each case, and the small dots represent Fe_3O_4 nanoparticles. (f–k) Cross-section SEM images of the GO–Fe_3O_4–SiO_2 aerogels prepared in the presence of a magnetic field. GO, $\sim$4 mg mL^{-1}; Fe_3O_4 : GO mass ratio, $\sim$1.3 : 1; in butyl acetate; magnetic field $\sim$4500 G (0.45 T).

ascribed to the planar anchoring of GO nanosheets at the liquid–glass wall interface, which causes the nanosheets near the interface to orient parallel to the surface of the cuvette without an external field. The GO liquid crystalline domains near the interface therefore are perpendicular to the viewing direction, contributing to the blue light reflection.

Interestingly, when the magnet was positioned behind the samples, the blue color of the GO–Fe_3O_4 hydrophobic photonic liquids disappeared when viewed along the direction of the magnetic field but remained visible when viewed normal to the field direction (Fig. 1e). It appears that introducing the magnet causes the GO liquid crystalline domains to reorient parallel to

the field direction so that the normal vector of the plane of the sheets is reoriented away from the viewing direction, thus leading the blue color to be no longer observable from the original, parallel viewing angle (Fig. 1a and e). Previous studies have also shown that polystyrene spheres in a magnetized ferrofluid tended to form a chain-like structure arranged parallel to the field direction.[47] This behavior implies that particles less magnetizable than their surrounding medium appear to have a magnetic moment antiparallel to the magnetic field, and can be oriented by magnetic fields. It is possible that GO nanosheets also reorient their planes in response to the magnetization of ferrofluid. The normal of each nanosheet is likely degenerately distributed in the plane perpendicular to the magnetic field (Fig. 1a–c). It is worth noting that $GO-Fe_3O_4$ aqueous photonic liquids also exhibited similar color disappearance in response to a magnetic field (Fig. S7, ESI†), although the aqueous samples showed relatively weak stability (Fig. S4, ESI†) and phase separation (Fig. S8, ESI†) over time.

To visualize the effect of magnetic field on the orientation of GO nanosheets, we made aerogels that captured the structures within the suspensions according to our previous studies.[44,45,62] We exploited the hydrolysis and condensation of tetramethyl orthosilicate into silica gel, or gelation of cellulose nanocrystal (CNC) suspensions induced by solvent-exchange, to immobilize $GO-Fe_3O_4$ and $GO-CNC-Fe_3O_4$ aqueous suspensions in the presence or absence of a magnetic field to produce $GO-SiO_2-Fe_3O_4$ and $GO-CNC-Fe_3O_4$ gels, and then converted them to alcogels by solvent exchange with ethanol. These alcogels were subsequently solidified by supercritical CO_2 drying to yield $GO-SiO_2-Fe_3O_4$ and $GO-CNC-Fe_3O_4$ aerogels for scanning electron microscopy (SEM) imaging. Cross-sectional SEM images of the $GO-SiO_2-Fe_3O_4$ aerogels showed layered structures, in which the GO layers were aligned nearly parallel to the direction of the magnetic field (Fig. 1f–k). In the $GO-CNC-Fe_3O_4$ aerogels, the cross-sectional areas were mostly covered by CNCs due to the high CNC concentration required to induce gelation in the suspensions (Fig. S9 and S10, ESI†). However, it was clearly observed that the diamagnetic CNCs also aligned nearly parallel to the magnetic field (Fig. S10, ESI†). The energy-dispersive X-ray (EDX) mapping images of the $GO-SiO_2-Fe_3O_4$ aerogel indicated a uniform distribution of Fe_3O_4 nanoparticles (NPs) in the chosen areas (Fig. S11, ESI†).
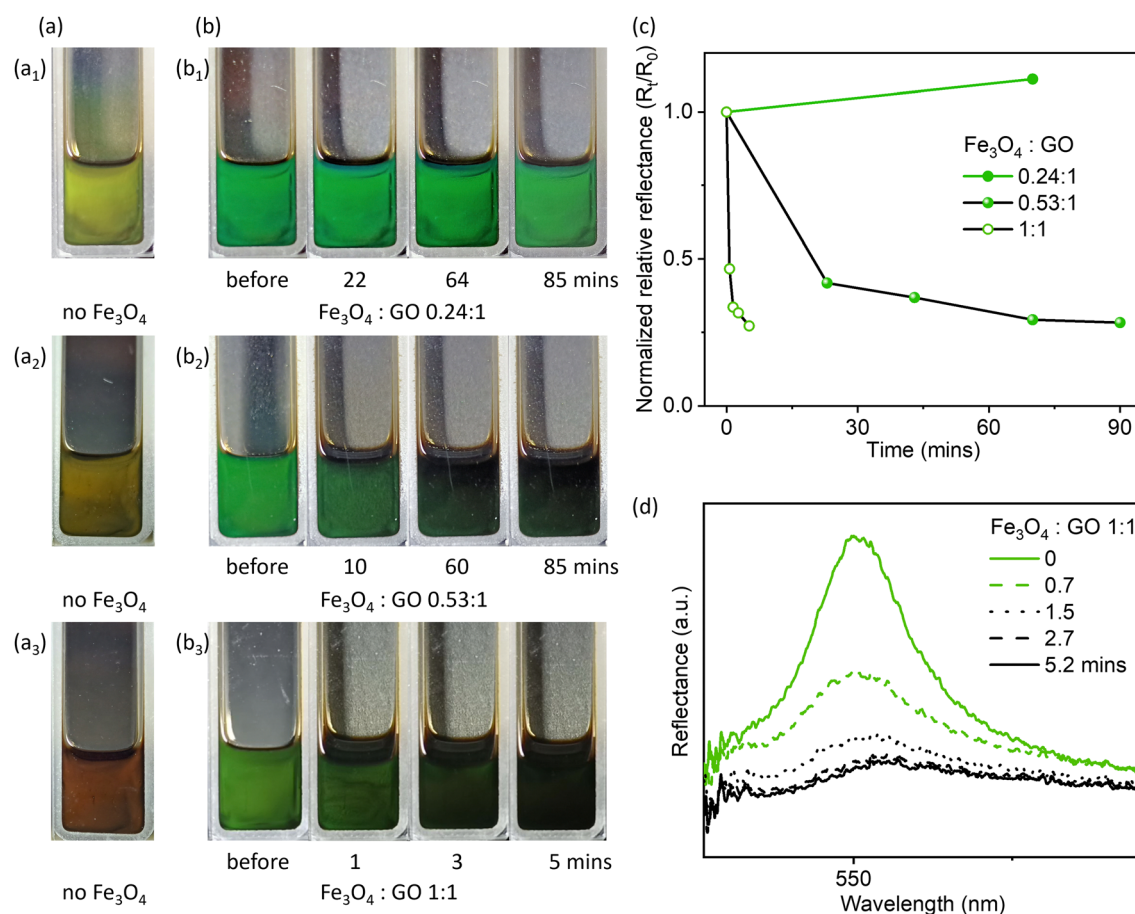

Fig. 2 (a) Photographs of GO hydrophobic photonic liquids with different colors in butyl acetate (a_1-yellow $\sim$5 mg mL^{-1} GO, a_2-sunset yellow $\sim$4.5 mg mL^{-1} GO, a_3-red $\sim$3.5 mg mL^{-1} GO) prior to adding Fe_3O_4 NPs. (b) The colors of the liquids were tuned to green by controlling the Fe_3O_4 : GO ratio ($b_1 \sim$0.24 : 1, $b_2 \sim$0.53 : 1, $b_3 \sim$1 : 1), and were switched off with a magnetic field ($\sim$4500 G). (c) Normalized relative reflectance spectra of the $GO-Fe_3O_4$ hydrophobic photonic liquids in response to a magnetic field at different times. (d) Reflection spectra of the $GO-Fe_3O_4$ photonic liquids shown in b_3 responding to a magnetic field with increasing time. The sample shown with the word "before" in (b) is a photograph of the suspension before applying a magnetic field.

However, the detected concentration of these Fe_3O_4 NPs is relatively low. This could be due to prolonged exposure to the magnetic field, coupled with the presence of thick SiO_2 layers and Au/Pd sputter coating layers on the Fe_3O_4 surface, which may have masked the nanoparticles. For comparison, aerogels prepared by the same methods in the absence of an applied magnetic field did not show obvious particle alignment (Fig. S12, ESI†). Based on the alignment of nonmagnetic particles shown in SEM images (Fig. 1f–k and Fig. S9, S10, ESI†), and the optical phenomenon shown in Fig. 1e, we believe that GO nanosheets in the magnetized ferrofluids are oriented parallel to the applied magnetic field, providing opportunities to switch off or restore the reflection colors.

The Fe_3O_4 concentration and Fe_3O_4:GO mass ratios are important for creating the magnetic field-responsive photonic liquids. To investigate the effect of Fe_3O_4 concentration, we prepared GO–Fe_3O_4 hydrophobic photonic liquids (Fig. 2) with varying Fe_3O_4 concentration and Fe_3O_4:GO mass ratios, which simultaneously change the reflection colors of GO-only hydrophobic photonic liquids as shown in Fig. 2a to green due to the depletion interaction between particles as mentioned above (Fig. S5, ESI†). The magnet was positioned behind the photonic liquids to create a magnetic field ($\sim$4500 G) perpendicular to the front side of the cuvette. At low Fe_3O_4:GO mass ratio (0.24:1), no obvious color changes were observed (Fig. 2b$_1$) even after 80 min, similar to observations of pure GO hydrophobic photonic liquids (Fig. S13, ESI†).

However, by increasing the Fe_3O_4:GO mass ratio to 0.53:1, the green color of the reflective liquid gradually faded in response to the magnetic field, and only a very pale green color remained after $\sim$60 mins (and Fig. 2b$_2$). We then further increased the Fe_3O_4:GO mass ratio to 1:1, and found that the higher Fe_3O_4 concentration could significantly reduce the time for turning off the reflection color, as indicated by the fast reduction in R_t/R_0 (Fig. 2b$_3$, c and d, R_0 is the normalized reflectance of samples before cycling test, R_t is the normalized reflectance at a given time).

Moreover, when the Fe_3O_4 concentration and the Fe_3O_4:GO ratio were sufficiently high (3.5 mg mL^{-1} for GO concentration and 1:1 for mass ratio), the optical properties could also respond even under a weaker magnetic field (adjusted by controlling the distance between the magnet and sample, Fig. S14, ESI†), though this process was slow (Fig. 3 and Fig. S15, ESI†). Under a weak magnetic field of $\sim$460 G, the visible light reflection was significantly weakened, but a pale green color was still visible (Fig. 3a$_2$ and b), indicating a relatively low extent of domain reorientation in response to the weak magnetic field. It is likely that the diamagnetic response of GO domain reorientation requires a continuous magnetized ferrofluid environment around the GO liquid crystalline domains. Once such an environment is established, the extent of magnetoresponsive photonic properties can be tuned by further carefully varying the field strength or Fe_3O_4 concentration.

The reflection colors could be restored by removing the magnetic fields, by altering the field direction (*i.e.*, moving the magnet from behind the cuvette to beside it to create a magnetic field perpendicular to the viewing direction), or by applying additional force (*e.g.*, shaking, vortexing), thereby allowing for on/off switching of reflection colors (Fig. 4). Compared to the cycling test of photonic liquids where the magnetic field was repeatedly introduced and removed (Fig. 4d and Fig. S16b, ESI†), samples where the field direction was cycled (Fig. 4d and Fig. S16a, ESI†) showed more obvious color restoration, as indicated by a higher R_t/R_0 (Fig. 4d and Fig. S16, ESI†). Also, the time required for color restoration was shorter in the presence of a magnetic field than without it, leading to a shorter completion time for 10 cycles. We also observed that after several cycles, it took longer to switch off the reflection colors, and a few striped areas still appeared faint green (Fig. S16, ESI†). Although the reasons for this are still unclear, they may be related to the spatial distribution of Fe_3O_4 NPs or the microphase separation between GO and Fe_3O_4, caused by the magnet. We could avoid these issues by applying additional force such as shaking or vortexing. This allows for restoration of the reflection colors immediately during the cycling test, and significantly reduced the cycling time (Fig. 4d).
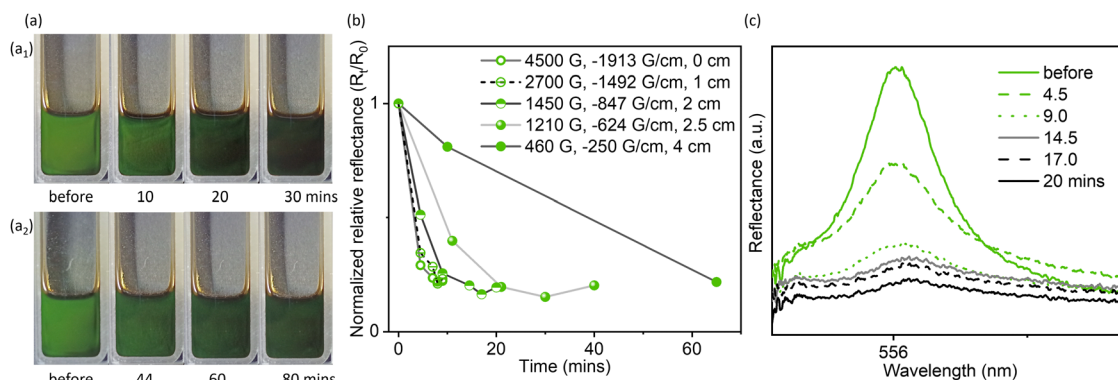

Fig. 3 (a) Photographs of the green hydrophobic GO–Fe_3O_4 photonic liquids (mass ratio, $\sim$1:1; in butyl acetate) in response to decreasing magnetic fields at different times (1450 G for a$_1$ and 460 G for a$_2$). (b) Normalized relative reflectance of the GO–Fe_3O_4 photonic liquids in response to field strength at different times. (c) Reflection spectra of the green hydrophobic GO–Fe_3O_4 photonic liquids shown in a$_1$ in response to a 1450 G magnetic field with increasing time. The magnet was positioned behind the samples.
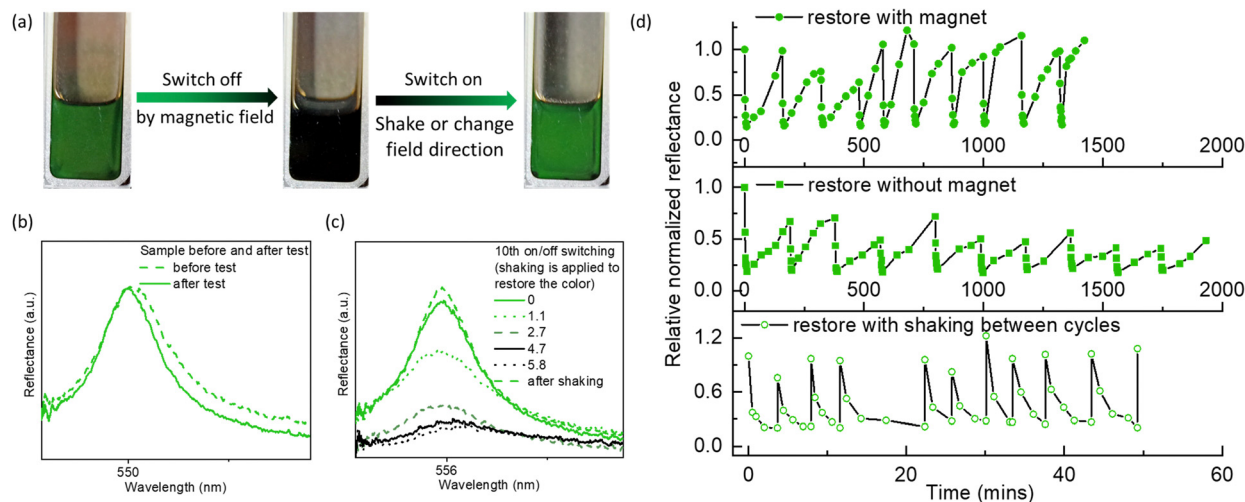
Fig. 4 (a) Photograph showing the reversible color change of a GO−Fe$_3$O$_4$ hydrophobic photonic liquid. The color restoration is achieved by adjusting the magnetic field direction or a vortex shaker. The process of switching off and on control by magnetic field can be seen in Videos S1 and S2 (ESI†). (b) Reflection spectra of the GO−Fe$_3$O$_4$ hydrophobic photonic liquid before and after cycling test. (c) Cycling test for the on/off switch of reflection colors of GO−Fe$_3$O$_4$ hydrophobic photonic liquids. (d) Time-dependent reflection spectra of the green hydrophobic GO−Fe$_3$O$_4$ photonic liquids for the 10th cycling (shaking was applied to expedite color restoration). The concentration of GO is ∼3.5 mg mL^{-1} in butyl acetate and the mass ratio of Fe$_3$O$_4$: GO is ∼1 : 1. The magnetic field is ∼4500 G.

Conclusions

In conclusion, we developed a switchable photonic liquid based on the diamagnetic response of GO nanosheets in a magnetized ferrofluid. GO nanosheets can be reoriented parallel to the field direction in response to the magnetization of the ferrofluid environment, as indicated by the anisotropic optical properties shown from the samples in a rectangular cuvette. The reflection colors of these reflective liquids can be switched on or off by adjusting the direction of the magnetic field, or by introducing and removing a magnetic field. This method avoids the use of superconducting magnets, and has the potential to be extended to other lyotropic photonic systems of shape-anisotropic nano-particles, where the liquid environment can be modified by introducing magnetic additives.

Author contributions

Y. T. X. and M. J. M. conceived the project. Y. T. X. designed and conducted most of the experiments and wrote the first draft of the manuscript. A. J. A. helped with the graphene oxide preparation and performed SEM experiments. A. M. performed TEM experiments. M. O. measured and analyzed the magnetic properties of Fe$_3$O$_4$ NPs. M. J. M. contributed to interpretation of the results and discussed the project extensively with the other co-authors. All of the authors contributed to the refine-ment and editing of the manuscript.

Conflicts of interest

The authors declare no conflict of interest.

Acknowledgements

References

1 P. Vukusic and J. R. Sambles, *Nature*, 2003, **424**, 852–855.
2 L. Shang, W. Zhang, K. Xu and Y. Zhao, *Mater. Horiz.*, 2019, **6**, 945–958.
3 J. Teyssier, S. V. Saenko, D. van der Marel and M. C. Milinkovitch, *Nat. Commun.*, 2015, **6**, 6368.
4 D. Gur, B. A. Palmer, B. Leshem, D. Oron, P. Fratzl, S. Weiner and L. Addadi, *Angew. Chem., Int. Ed.*, 2015, **54**, 12426–12430.
5 J. H. Holtz and S. A. Asher, *Nature*, 1997, **389**, 829–832.
6 Y. F. Yue, M. A. Haque, T. Kurokawa, T. Nakajima and J. P. Gong, *Adv. Mater.*, 2013, **25**, 3106–3110.
7 Z. Li, Q. Fan and Y. Yin, *Chem. Rev.*, 2022, **122**, 4976–5067.
8 Q. Fu, W. Yu, G. Bao and J. Ge, *Nat. Commun.*, 2022, **13**, 7007.
9 J. J. Walish, Y. Kang, R. A. Mickiewicz and E. L. Thomas, *Adv. Mater.*, 2009, **21**, 3078–3081.
10 M. Stefik, S. Guldin, S. Vignolini, U. Wiesner and U. Steiner, *Chem. Soc. Rev.*, 2015, **44**, 5076–5091.
11 B. M. Boyle, T. A. French, R. M. Pearson, B. G. McCarthy and G. M. Miyake, *ACS Nano*, 2017, **11**, 3052–3058.
12 M. Poutanen, G. Guidetti, T. I. Gröschel, O. V. Borisov, S. Vignolini, O. Ikkala and A. H. Gröschel, *ACS Nano*, 2018, **12**, 3149–3158.

13 G. H. Lee, T. M. Choi, B. Kim, S.-H. Han, J. M. Lee and S. H. Kim, *ACS Nano*, 2017, **11**, 11350–11357.

14 H. Wang, Y. Liu, Z. Chen, L. Sun and Y. Zhao, *Sci. Adv.*, 2020, **6**, eaay1438.

15 L. Zhou, J. Fei, W. Fang, L. Shao, Q. Liu, H. He, M. Ma, Y. Shi, S. Chen and X. Wang, *Nanoscale Horiz.*, 2022, **7**, 890–898.

16 C. I. Aguirre, E. Reguera and A. Stein, *Adv. Funct. Mater.*, 2010, **20**, 2565–2578.

17 J. Lee, Y. Jung, M. Lee, J. S. Hwang, J. Guo, W. Shin, J. Min, K. R. Pyun, H. Lee, Y. Lee, J. Shiomi, Y.-J. Kim, B.-W. Kim and S. H. Ko, *Nanoscale Horiz.*, 2022, **7**, 1054–1064.

18 X. Xu, G. Friedman, K. D. Humfeld, S. A. Majetich and S. A. Asher, *Adv. Mater.*, 2001, **13**, 1681–1684.

19 J. Ge, Y. Hu and Y. Yin, *Angew. Chem., Int. Ed.*, 2007, **46**, 7428–7431.

20 B. Frka-Petesic, G. Guidetti, G. Kamita and S. Vignolini, *Adv. Mater.*, 2017, **29**, 1701469.

21 M. Anyfantakis, V. S. R. Jampani, R. Kizhakidathazhath, B. P. Binks and J. P. F. Lagerwall, *Angew. Chem., Int. Ed.*, 2020, **59**, 19260–19267.

22 G. Kamita, S. Vignolini and A. G. Dumanli, *Nanoscale Horiz.*, 2023, **8**, 887–891.

23 J.-B. Moon, S.-J. Lee, S.-H. Kim, Y. Chang, H. Hwang and G.-R. Yi, *Chem. Mater.*, 2022, **34**, 7897–7905.

24 D. Gur, Y. Politi, B. Sivan, P. Fratzl, S. Weiner and L. Addadi, *Angew. Chem., Int. Ed.*, 2013, **52**, 388–391.

25 L. M. Mäthger, M. F. Land, U. E. Siebeck and N. J. Marshall, *J. Exp. Biol.*, 2003, **206**, 3607–3613.

26 P. J. Herring, *Comp. Biochem. Phys. A*, 1994, **109**, 513–546.

27 J.-C. P. Gabriel, F. Camerel, B. J. Lemaire, H. Desvaux, P. Davidson and P. Batail, *Nature*, 2001, **413**, 504–508.

28 P. Davidson, C. Penisson, D. Constantin and J.-C. P. Gabriel, *Proc. Natl. Acad. Sci. U. S. A.*, 2018, **115**, 6662–6667.

29 K. El Rifaii, H. H. Wensink, C. Goldmann, L. Michot, J.-C. P. Gabriel and P. Davidson, *Soft Matter*, 2021, **17**, 9280–9292.

30 M. Wong, R. Ishige, T. Hoshino, S. Hawkins, P. Li, A. Takahara and H.-J. Sue, *Chem. Mater.*, 2014, **26**, 1528–1537.

31 T.-Z. Shen, K. N. A. Perera, A. R. Masud, P. A. N. S. Priyadharshana, J.-Y. Park, Q.-H. Wang, S.-H. Hong and J.-K. Song, *Cell Rep. Phys. Sci.*, 2023, **4**, 101343.

32 Y. Wang, X. Kan, Y. Liu, J. Ju and X. Yao, *Nanoscale*, 2023, **15**, 9060–9068.

33 K. Sano, Y. S. Kim, Y. Ishida, Y. Ebina, T. Sasaki, T. Hikima and T. Aida, *Nat. Commun.*, 2016, **7**, 12559.

34 E. Mouri, C. Ogami, T. Fukumoto and T. Nakato, *Chem. Lett.*, 2020, **49**, 717–720.

35 W. Yang, S. Yamamoto, K. Sueyoshi, T. Inadomi, R. Kato and N. Miyamoto, *Angew. Chem., Int. Ed.*, 2021, **60**, 8466–8471.

36 P. H. Michels-Brito, V. Dudko, D. Wagner, P. Markus, G. Papastavrou, L. Michels, J. Breu and J. O. Fossum, *Sci. Adv.*, 2022, **8**, eabl8147.

37 N. Miyamoto and S. Yamamoto, *ACS Omega*, 2022, **7**, 6070–6074.

38 V. Dudko, O. Khoruzhenko, S. Weiss, M. Daab, P. Loch, W. Schwieger and J. Breu, *Adv. Mater. Technol.*, 2023, **8**, 2200553.

39 J. I. Paredes, S. Villar-Rodil, A. Martinez-Alonso and J. M. D. Tascon, *Langmuir*, 2008, **24**, 10560–10564.

40 J. E. Kim, T. H. Han, S. H. Lee, J. Y. Kim, C. W. Ahn, J. M. Yun and S. O. Kim, *Angew. Chem., Int. Ed.*, 2011, **50**, 3043–3047.

41 Z. Xu and C. Gao, *ACS Nano*, 2011, **5**, 2908–2915.

42 P. Li, M. Wong, X. Zhang, H. Yao, R. Ishige, A. Takahara, M. Miyamoto, R. Nishimura and H.-J. Sue, *ACS Photonics*, 2014, **1**, 79–86.

43 S.-H. Hong, T.-Z. Shen and J.-K. Song, *Opt. Express*, 2015, **23**, 18969–18974.

44 Y.-T. Xu, U. V. Mody and M. J. MacLachlan, *Nanoscale*, 2021, **13**, 7558–7565.

45 Y.-T. Xu, J. Li and M. J. MacLachlan, *Nanoscale Horiz.*, 2022, **7**, 185–191.

46 L. Wu, M. Ohtani, M. Takata, A. Saeki, S. Seki, Y. Ishida and T. Aida, *ACS Nano*, 2014, **8**, 4640–4649.

47 A. T. Skjeltorp, *Phys. Rev. Lett.*, 1983, **51**, 2306–2309.

48 C. Ooi, R. M. Erb and B. B. Yellen, *J. Appl. Phys.*, 2008, **103**, 07E910.

49 B. B. Yellen, O. Hovorka and G. Friedman, *Proc. Natl. Acad. Sci. U. S. A.*, 2005, **102**, 8860–8864.

50 R. M. Erb, H. S. Son, B. Samanta, V. M. Rotello and B. B. Yellen, *Nature*, 2009, **457**, 999–1002.

51 L. He, Y. Hu, H. Kim, J. Ge, S. Kwon and Y. Yin, *Nano Lett.*, 2010, **10**, 4708–4714.

52 L. He, M. Wang, Q. Zhang, Y. Lu and Y. Yin, *Nano Lett.*, 2013, **13**, 264–271.

53 A. Al Harraq, J. G. Lee and B. Bharti, *Sci. Adv.*, 2020, **6**, eaba5337.

54 A. Al Harraq, A. A. Hymel, E. Lin, T. M. Truskett and B. Bharti, *Commun. Chem.*, 2022, **5**, 72.

55 F. Yang, F. Mou, Y. Jiang, M. Luo, L. Xu, H. Ma and J. Guan, *ACS Nano*, 2018, **12**, 6668–6676.

56 W. S. Hummers, Jr. and R. E. Offeman, *J. Am. Chem. Soc.*, 1958, **80**, 1339.

57 G. Wang, X. Zhang, A. Skallberg, Y. Liu, Z. Hu, X. Mei and K. Uvdal, *Nanoscale*, 2014, **6**, 2953–2963.

58 M. D. Nguyen, H.-V. Tran, S. Xu and T. R. Lee, *Appl. Sci.*, 2021, **11**, 11301.

59 C. Sotebier, A. Michel and J. Fresnais, *Appl. Sci.*, 2012, **2**, 485–495.

60 S. Asakura and F. Oosawa, *J. Chem. Phys.*, 1954, **22**, 1255–1256.

61 M. Adams, Z. Dogic, S. L. Keller and S. Fraden, *Nature*, 1998, **393**, 349–352.

62 Y.-T. Xu, Y. L. Dai, T.-D. Nguyen, W. Y. Hamad and M. J. MacLachlan, *Nanoscale*, 2018, **10**, 3805–3812.